Earthquake Geotechnical Engineering for Protection and Development of Environment and Constructions – Silvestri & Moraci (Eds)
© 2019 Associazione Geotecnica Italiana, Rome, Italy, ISBN 978-0-367-14328-2

Effectiveness of sheet pile as a seismic retrofit for piled abutment subjected to liquefaction-induced lateral spreading

P. Saha, K. Horikoshi & A. Takahashi
Tokyo Institute of Technology, Meguro, Tokyo, Japan

ABSTRACT: This paper presents the numerical simulation of a large-scale shake table experiment carried out by Public Works Research Institute (PWRI), Japan. The experiment is conducted to observe the seismic response of a pile-supported bridge abutment in which the sheet pile is used as a seismic retrofit against lateral spreading. The model abutment both in shake table test and simulation is designed according to the old Japanese standards for Highway Bridges. The numerical results confirm that the installation of sheet pile minimizes the kinematic demand of the existing piles. A series of finite element analyses have been performed to determine the effect of the stiffness of sheet pile on the seismic performance of the piled abutment. The parametric study shows that the increase of bending stiffness of sheet pile up to some level increases its efficiency in reducing the bending moment of existing piles during lateral spreading.

1 INTRODUCTION

Old bridge abutment resting on a liquefiable soil are seriously vulnerable to get damaged by the ground displacement and demand to develop appropriate retrofitting techniques against lateral spreading. Many effective ground improvement techniques have been developed to mitigate liquefaction-induced ground failure. However, the liquefaction mitigation near the existing structures is still a burning issue to the geotechnical engineers. The use of sheet pile to prevent liquefaction-induced ground displacement have been studied before (Li & Motamed 2017 and Rasouli et al. 2014) and recommended as a potential remedial measure in this regard. However, the sheet piles as a seismic retrofit for the existing piled abutment, which has not been studied before, is the main focus of this paper. The principle of using sheet pile is to prevent the lateral movement of the soil thus reducing the kinematic demand of the existing structures.

This paper presents the two-dimensional finite element analysis of a large-scale shake table experiment conducted by PWRI in which sheet pile is used to prevent the lateral flow of the ground. The finite element analysis can reasonably simulate the overall response of the ground which validates the use of this finite element code for further parametric study. Both the numerical and experimental results show that the sheet pile can reduce the bending moment of the existing piles. Several parametric studies have also been performed in order to determine the effect of length of the sheet pile extended into the non-liquefiable crustal layer and the stiffness of the sheet pile itself. No significant change in the response of the existing piles is observed when the sheet piles are extended inside the crustal layer. However, the increase of bending stiffness of sheet pile up to some level increases its efficiency in reducing the bending moment of existing piles during lateral spreading.

2 DESCRIPTION OF THE SHAKE TABLE EXPERIMENT

A large-scale shake table experiment is conducted by PWRI in order to determine the efficiency of sheet pile as a seismic retrofit for piled abutment resting on liquefiable soil. The experimental model consists of a pile-supported bridge abutment along with an approach embankment

resting on liquefiable foundation soil. The model is prepared inside a large steel container having the dimensions of 6 m × 3 m × 2 m which is rigidly attached to the shake table. A sheet pile is installed in front of the abutment in the channel side to prevent lateral spreading.

2.1 *Preparation of the model ground*

Silica Sand No. 6 with a relative density of 50% is used to make the embankment as well as the foundation soil which are placed over a 100 mm thick drainage layer. The specific gravity of soil solids is 2.647, and the maximum and minimum void ratio are 1.014 and 0.594 respectively. The coefficient of permeability of the model ground is 5.15×10^{-4} m/s. The dry deposition method is used to prepare the model ground and then compacted by tamping to reach up to the desired level of compaction. The foundation soil up to the base of the pile cap is kept saturated to ensure liquefaction of that soil during shaking.

2.2 *Description of the sheet pile and the abutment*

The model abutment is designed according to the old Japanese standard for highway bridges (Japan Road Association 1964) following a scaling ratio of 1:10. Half-width of the abutment is modeled in order to get the advantage of symmetry which is supported by twelve piles arranged in three rows as shown in Figure 1. The piles are designed with a 1.10 m long steel (SS400) bar having a cross-sectional dimension of 19 mm × 8 mm in order to adjust to the bending stiffness of the pile design based on the old design standard. A series of a circular ring having an outer diameter of 48.6 mm are attached to the pile along its length to impose the effect of the volume of the piles. The head of the piles is rigidly connected to the footing of the abutment whereas the tips are hinged with the container in order to prevent the translational movement during shaking. The embankment is observed to colloid with the bridge girder during the seismic motion which substantially influences the response of the abutment and needs to be modeled. A horizontal strut rigidly attached to the container is placed in front of the upper part of the abutment maintaining a gap of 5 mm in order to simulate the effect of the bridge girder. It is already mentioned that a sheet pile is used as an indirect reinforcement to prevent lateral spreading. The sheet pile having the equal width of the abutment is placed in front of the abutment in the channel side fixed with the container at its base. The specifications of the model abutment and the sheet pile are tabulated in Table 1.

3 FINITE ELEMENT ANALYSIS

Finite element analysis is nowadays a useful tool to predict the response of soil subject to seismic loading. In this study, two-dimensional finite element analyses have been conducted in order to determine the response of piled abutment subjected to liquefaction induced lateral spreading and the feasibility of sheet pile as a seismic retrofit against lateral spreading. The finite element code developed by Takahashi (2002) is used to simulate the shake table experiment conducted by PWRI. A fully coupled u-p formulation is used in this code. The governing equations together with constitutive formulations have been used here to define the response of a porous media.

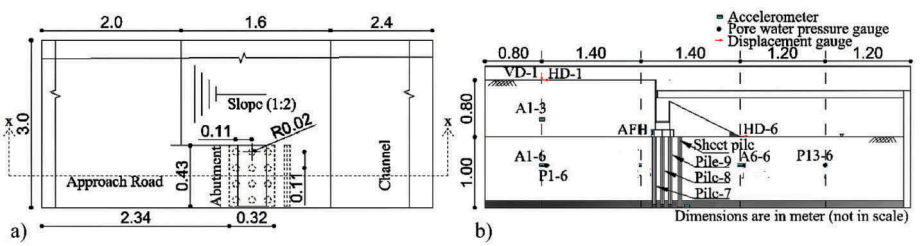

Figure 1. Experimental model: (a) aerial view and (b) x-x section of the aerial view.

Table 1. Physical properties of piles and sheet pile

Element type		Properties
Pile upholding (each pile)	Dimensions (mm)	1102×19×8
	Modulus of elasticity (N/m^2)	2×10^{11}
	Mass (kg)	1.31
	Outer diameter (mm)	48.6
	Inner diameter (mm)	46.6
Circular ring (each pile)	Height (mm)	846
	Material	Steel (SUS304)
	Mass (kg)	2.0
Sheet pile	Flexural rigidity "EI" ($N.mm^2$)	3.9×10^{10}

3.1 *Numerical model and boundary condition*

Two-dimensional finite element analysis is usually conducted under plane strain condition which is considered as a limitation of this technique to model a structure having a finite width in the transverse direction. However, because of its less computational demand with reasonable accuracy, two-dimensional finite element analysis is used herein these analyses. It is simplified that the extended part of the embankment width does not have significant effect on the structural response. Therefore, the width of the embankment is considered as the equal width of the abutment which imposes a three-dimensional essence in a two-dimensional analysis. A master and slave node technique is used which impose an identical deformation between the nodes of the structural elements and the corresponding linked nodes of the soil element.

In order to model the piles in plane strain condition, the bending stiffness of four piles in a row in the experiment is estimated as the bending stiffness of the representative pile for that row in the numerical model. Boundary conditions in the numerical model are imposed in such a way that it can simulate the experimental boundary conditions. All kinds of movement of the nodes are restricted at the bottom boundary. The nodes along the vertical boundary are kept free to move vertically during the analysis whereas, the horizontal movement is restricted. All other nodes are set free against translational and vertical movement. In order to simulate the effect of the bridge girder, the node of the abutment that comes into contact with the strut is restricted to move horizontally. Besides, the fluid flow velocity in the horizontal direction at the boundaries of the analytical domain are set to zero. All kind of fluid flow through the sheet pile is restricted since the sheet pile also prevents the flow of fluid in reality.

3.2 *Material parameters*

The model ground is defined as an elastoplastic material and designed with four-node solid elements. The constitutive model proposed by Asaoka et al. (2002) is used to predict the cyclic response of soil. The constitutive model is formulated with seventeen parameters out of which κ and λ are the tangent of the swelling and the normal compression line and can be determined from consolidation test. e_o, ν, and G_s are respectively the initial void ratio, Poisson's ratio and specific gravity of the soil which can be determined from element tests. All other parameters are determined by trial and error so that the numerical liquefaction resistance curve closely fits the experimental one. Two different sets of parameters are used to define the low liquefiable soil (LLS) and highly liquefiable soil (HLS). The comparison of the liquefaction resistance curves obtained from experiment and numerical results using two sets of parameters is shown in Figure 2a. The typical stress path and stress-strain curve under cyclic loading are shown in Figure 2b. The parameters for LLS and HLS are listed in Table 2. Besides, the abutment is modeled as four-node elastic solid elements and the piles and sheet piles are designed as elastic beam elements. It is unlikely the piles behave elastically in reality rather some plastic hinge may develop which may cause excessive rotation which is beyond the scope of this study. Therefore, all the structural elements in this study are regarded as perfectly elastic material. The parameters of the structural elements are listed in Table 3.

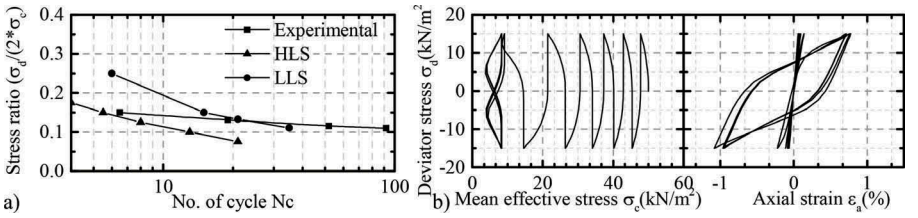

Figure 2. a) Comparison of experimental and numerical liquefaction resistance curve, and b) typical stress path and stress-strain curve under cyclic loading for HLS.

Table 2. Parameters for LLS and HLS

Parameters	LLS	HLS
κ	0.004	0.004
λ	0.05	0.05
e_o	0.804	0.804
ν	0.33	0.33
φ	38.0	35.0
φ_d	30.0	38.0
b_r	5.0	3.0
m	2.75	0.1
a	1.0	2.7
R	0.85	1.0
R_o^*	1.0	0.25
K_o	1.0	1.0
k (m/sec)	5.14×10^{-04}	5.14×10^{-04}

Table 3. Parameters of structural elements.

Element type		Properties
Vertical wall	Density ρ (Mg/m^3)	1.59
	Modulus of elasticity E (N/m^2)	2×10^{11}
	Poisson's ratio ν	0.26
Footing	Density ρ (Mg/m^3)	2.10
	Modulus of elasticity E (N/m^2)	2×10^{11}
	Poisson's ratio ν	0.26
Pile	Flexural rigidity EI (N.m^2)	1.70×10^{3}
	Axial stiffness EA	31.92×10^{6}
Sheet pile	Flexural rigidity EI (N.m^2)	3.9×10^{4}

3.3 *Applied ground motion*

Seismic ground motion recorded during Tohoku Earthquake is applied in this experiment. The time period of earthquake motion is reduced with a factor $1/\sqrt{10}$ to follow the scaling law of time for 1g shake table experiments. However, acceleration time history recorded by an accelerometer which is attached to the base of the container during the experiment is used in this analysis as an input ground motion. The recorded data may contain background noise from different sources. Most of the noises are non-seismic and remain in the range of low or high frequency (Kramer 1996). This kind of high-frequency or low-frequency acceleration data which is beyond the engineering interest needs to be isolated from the recorded data. Another correction is also introduced to avoid the permanent displacement at the end of motion is commonly known as baseline correction. A computer-based software (Seismosignal-2016) is used for baseline correction and to

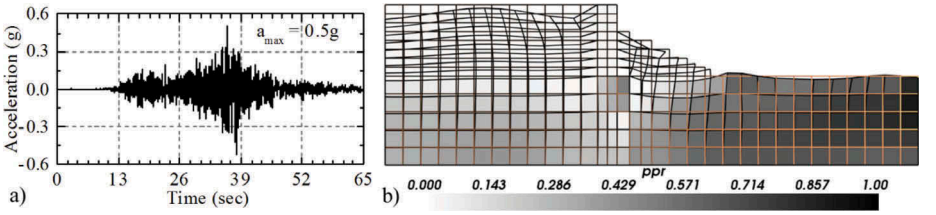

Figure 3. a) Input ground motion, and b) deformed shape of the model ground at 64.96 sec of shaking using LLS parameters.

obtain a bandpass filtered (frequencies in between 0.1 Hz to 25 Hz) ground motion data. The acceleration time history of input ground motion is shown in Figure 3a.

4 COMPARISON OF EXPERIMENTAL AND NUMERICAL RESULTS USING LLS PARAMETERS

The calculated deformed shape of the model ground almost at 64.96 sec is plotted in the frame of the original shape of the model ground as shown in Figure 3b. The picture presents clear evidence of lateral displacement of the ground towards the channel. Simultaneously, the surface of the embankment is observed to go under considerable settlement. The locations of the embankment near the outer boundary and the vertical wall of the abutment are observed to settle more than the surrounding areas. In these analyses, the periphery of the ground is modelled as a rigid boundary. Besides, the boundary conditions imposed on the abutment wall prevents its horizontal movement at the top. These boundary conditions instigate the pounding between the ground and those relatively rigid boundaries which may cause excessive settlement at that location resulting in a convex shape of the embankment surface. The comparison of the computed and measured displacement at different locations are illustrated in Figure 4.

4.1 *Generation of pore water pressure*

The comparison of computed and measured pore water pressure generation time history under the embankment and inside the channel is presented in Figure 5. The graph shows that the excess pore water pressure inside the channel (P13-6) almost reaches up to the initial effective stress denoted by the horizontal straight line ($r_u = 1.0$) both in experimental and numerical results which represents the liquefied state of the ground inside the channel. However, the calculated excess pore water pressure underneath the embankment, though follow the similar trend as that of the experimental results, is bigger in magnitude. None of the measured and calculated results at that location reaches up to the state of liquefaction under the embankment. Usually partially saturated soil exhibit delayed generation of pore water pressure and pretends like a dense soil. This kind of phenomenon is observed in the experimental results

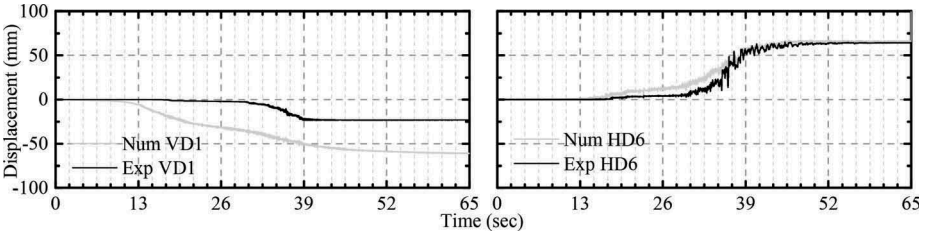

Figure 4. Comparison of measured and computed displacement of the ground at different locations using LLS parameters.

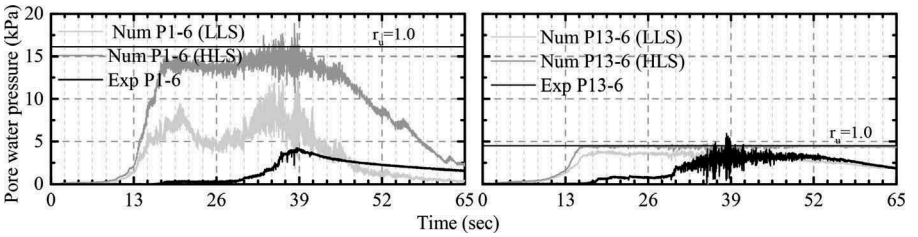

Figure 5. Pore water pressure generation time history.

which demonstrates the degree of saturation is not so high in the experiment. In order to simulate the seismic response of the partially saturated soil, the parameters (LLS) are selected in such a way so that it exhibits higher resistance against liquefaction. The LLS parameters can minimize the magnitude of excess pore water pressure to some extent in comparison with the excess pore water pressure obtained using HLS parameters as shown in Figure 5. However, the early generation of pore water pressure cannot be avoided.

4.2 *Ground response*

A comparison of computed and experimental acceleration time history at different locations is demonstrated in Figure 6. Although the peaks cannot be accurately simulated, the estimated acceleration is comparable with the measured values, especially in its development pattern. The measured acceleration time histories inside the channel show spiky peaks which cannot be simulated in the numerical results. Generally, this kind of spiky acceleration takes place because of the dilation during the cyclic shearing.

4.3 *Pile bending moment*

Both the experimental and numerical results confirm that the maximum bending moment takes place near the head of the pile and the pile-7 located at the backfill side is likely to experience the maximum bending moment. The bending moment profiles for pile-7, pile-8, and pile-9 are plotted while the maximum bending moment takes place near the head of pile-7 and compared with the measured values as shown in Figure 7a. The figure illustrates that the numerical results can reasonably simulate the bending moment of piles along with its distribution pattern. Pile-7 experiences maximum bending moment nearly at 38.21 sec in the experiment whereas it takes place at 38.22 sec in the numerical analysis. An increasing trend in bending moment near the head of the pile which is primarily caused by the kinematic earth pressure starts with the generation of excess pore water pressure and stops immediately after the dissipation phase starts (nearly at 39.00 sec) underneath the embankment. However, the maximum bending moment takes place immediately before that transition phase with the combination of kinematic and inertial earth pressure. Therefore, the early generation of pore water pressure in the numerical analysis may increase the magnitude of the bending moment however the maximum bending moment takes place nearly at the same time in the experiment and numerical analysis.

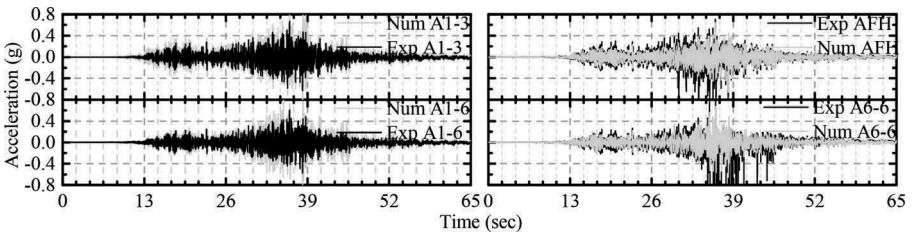

Figure 6. Comparison of computed and measured acceleration time history using LLS parameters.

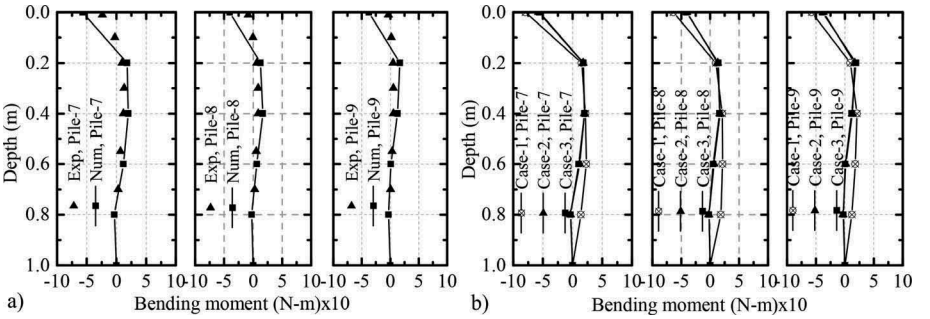

Figure 7. Comparison of a) computed and measured bending moment profiles of pile-7, pile-8, and pile-9 and b) bending moment profiles of pile-7, pile-8, and pile-9 in case-1, case-2, and case-3 where LLS parameters have been used for numerical analysis.

5 EFFICIENCY OF SHEET PILE

In order to determine the efficiency of the sheet pile as a seismic retrofit two additional finite element (FE) models have been analyzed. In the first FE model (case-1), the sheet pile has been omitted from the model (case-2) described in the preceding sections and in another FE model (case-3), the sheet pile has been extended into the non-liquefiable layer up to the slope surface. The primary purpose of installing sheet pile is to minimize the bending moment demand caused due to lateral spreading. Therefore, the capability of the sheet pile to reduce the bending moment of existing piles of the abutment is regarded as its efficiency in this study. The bending moment profiles of pile-7, pile-8, and pile-9 at 38.22 sec are plotted as described in the previous section for all the three cases and compared as illustrated in Figure 7b. It is worth-mentioning that LLS parameters have been used in these numerical analyses. The figure shows that the sheet pile can considerably reduce the bending moment although, the extension of the sheet pile inside the non-liquefiable layer does not have significant advantages over the sheet pile in case-2 where sheet pile is kept up to the liquefiable layer. Although the extension of sheet pile does not have any additional advantages in reducing bending moment, it is advantageous to some other natural disaster for example flooding or overflow of the river.

6 EFFECT OF STIFFNESS OF SHEET PILE

The severity of liquefaction depends on the state of liquefaction. The highly liquefiable soil is considered to be more hazardous than low liquefiable soil. Therefore, the effect of stiffness of the sheet pile on the response of existing piles resting both in LLS and HLS is described in this section. Besides, the experimental and the analytical results show that the absence of bridge girder during lateral spreading alters the bending moment distribution along the length of the pile. Excessively nonuniform lateral movement of soil may cause unseating bridge girder which leads the uninterrupted channel-ward movement of the abutment resulting the maximum bending moment near the head of the pile-9 which is located at the front face near the channel. Therefore, the maximum bending moment at the head of both pile-7 and pile-9 with the presence and absence of bridge girder is mostly focused in this section. In order to determine the effect of stiffness of sheet pile, several finite element analyses have been conducted with a varying bending stiffness of sheet pile from 0*EI to 5*EI. Where, 0*EI implies the FE model without any sheet pile and 5*EI represents the sheet pile stiffness five times of the sheet pile used in the experiment. All the analyses are conducted under both HLS and LLS conditions and the results are compared in Figure 8. The symbol “wg” and “ng” in the legend of Figure 8 indicates “with girder” and “no girder” respectively. Maximum bending moment in pile-7 and pile-9 takes place at a different time of the shaking depending on the existence of bridge girder and the level of liquefaction occurs in the analyses. Analyses result show a sharp

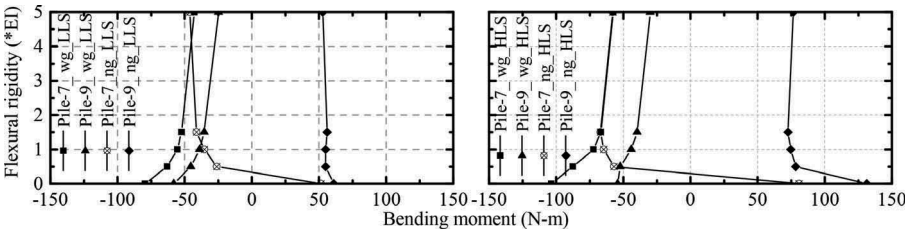

Figure 8. Effect of stiffness of sheet pile to prevent the failure of existing piles.

reduction in bending moment demand of the existing piles with increased stiffness of sheet pile up to 1.5*EI. Beyond this range, the rate of change of bending moment is considerably small. It implies that the efficiency of sheet pile to prevent lateral spreading does not proportionally increase with the increase of stiffness at the higher range. Therefore, a sheet pile having excessively large bending stiffness is probably less cost-effective in this regard.

7 CONCLUSION

This paper presents the effectiveness of the sheet pile as a seismic retrofit for piled abutment designed based on the old Japanese standard for highway bridges. A fully-coupled two-dimensional finite element analysis has been used to determine the seismic response. The analytical results show that the finite element analysis can capture the overall response of the model ground and the structure as well. The following conclusions can be drawn from the analytical results.

Installation of sheet pile can considerably reduce the bending moment demand of the existing piles of the abutment during lateral spreading.

The extension of sheet pile inside the non-liquefiable layer of the embankment does not show any additional advantages on the seismic performance of the abutment. However, it is recommended for ease of installation and better maintenance during flooding.

Increase in stiffness of sheet pile increases its efficiency as a seismic retrofit for the piled abutment up to a certain range. However, the efficiency of sheet pile to prevent lateral spreading does not proportionally increase with the increase of stiffness at a higher range.

ACKNOWLEDGEMENT

The authors would like to acknowledge the contribution of Public Works Research Institute in this study by allowing us to use their experimental results.

REFERENCES

Antoniou, S. & Pinho, R., 2016. SeismoSignal.

Asaoka, A. et al., 2002. An elasto-plastic description of two distinct volume change mechanisms of soils. *Soils and Foundations*, 42(5),pp.47–57.

Japan Road Association, 1964. Design guideline for substructures for highway bridges.

Kramer, S.L., 1996. *Geotechnical Earthquake Engineering*, Pearson Education India.

Li, G. & Motamed, R., 2017. Finite element modeling of soil-pile response subjected to liquefaction-induced lateral spreading in a large-scale shake table experiment. *Soil Dynamics and Earthquake Engineering*, 92, pp.573–584.

Rasouli, R., Towhata, I. & Rattez, H., 2014. Shaking table model tests on mitigation of liquefaction-induced distortion of shallow foundation. In *6th Japan-Taiwan Joint Workshop on Geotechnical Hazards from Large Earthquakes and Heavy Rain falls*.

Takahashi, A., 2002. Soil – pile interaction in liquefaction-induced lateral spreading of soils. *DEng. dissertation, Tokyo Institute of Technology*.